XVII IMEKO World Congress
Metrology in the 3rd Millennium
June 22–27, 2003, Dubrovnik, Croatia

ON THE BEHAVIOUR OF IN-FIBRE BRAGG GRATING SENSORS FOR STRAIN MEASUREMENT ON PLANE AND CURVED SURFACES

Leonardo D'Acquisto[1], *Roberto Montanini*[2]

[1] Dipartimento di Meccanica, University of Palermo, Italy
[2] Dipartimento di Chimica Industriale ed Ingegneria dei Materiali, University of Messina, Italy

Abstract – When compared with traditional electrical strain gauges used for strain monitoring, Fibre Bragg Grating (FBG) sensors have several distinguishing advantages that make them very attractive for many applications in different fields. Nevertheless, for practical applications, their metrological performance needs to be assessed under different operative conditions. In this paper attention has been focused on the response of FBGs when glued on a metallic surface that is not flat. Hollow-tube specimens with two different curvatures have been considered, together with a plane specimen used as reference. FBG signals were compared with those produced by electrical strain gauges. In addition, for the two hollow tube specimens, shadow moiré images of the specimen area between the FBG sensor and the strain gauge have been recorded in order to check the displacement field induced on the specimen. Preliminary results obtained show that the optical signal is markedly affected by the radius of curvature of the surface when the FBG sensor is bonded on a curved surface.

Keywords: FBG, strain measurements, shadow moiré

1. INTRODUCTION

In-fibre Bragg grating (FBG) sensors have undergone continuous and rapid development since they were first proposed for strain and temperature measurement about 10 years ago. The main reason for this is that FBG sensors have a number of distinguishing advantages over other implementations of fibre-optic sensors, including potentially low cost and unique wavelength-multiplexing capability, which makes them one of the most promising distributed sensor technologies for structural systems [1-3].

In-fiber Bragg grating sensors basically consist of a Ge-doped optical fibre segment in which a periodic modulation of the refractive index has been induced by exposing the core of the fibre to intense UV light. The basic principle of operation of an FBG-based sensor system lies in the dependence of the shift in wavelength of the returned Bragg signal on different measurands (e.g. strain, temperature, pressure, etc.). The strain response is due to both the physical elongation of the sensor and the change in fibre index due to photoelastic effects. Therefore, the Bragg wavelength shift may be expressed as a function of the applied strain and of the effective photoelastic coefficient.

The inherent wavelength-encoded output of Bragg gratings has a number of advantages over other sensing schemes [4]. One of the most important of these is that the output does not depend directly on total light levels, losses in the connecting fibres and couplers or source power.

On the other hand, as far as strain measurements are concerned, temperature–strain cross sensitivity due to the relative high level of thermal apparent strain manifested by FBG sensors has proven particularly difficult to eliminate and must be considered in the applications, through dummy gauges or more advanced dual-parameter fibre optic transducer design [5-6].

FBGs have shown considerable promise also for curvature measurements [7], particularly when the gratings are incorporated in special fibre types, including eccentric and multiple core types [8] and D-type fibres, in which the core is asymmetrically located relatively to the geometrical centre of the cross-centre of the cladding [9].

Owing to their small size, optical fibre gauges can be easily embedded unobtrusively into materials, particularly into composites already containing fibre reinforcements. However, when an optical fibre is embedded, the interpretation of the gauge response becomes more complex, due to the interface effects between the fibre and the material, as well as to multiple components of strain applied to the fibre [10-12]. The problem is further complicated when the strain field surrounding the gauge is not sufficiently uniform with respect to the gauge length [13] or when dynamic (cyclic) loading is involved [14].

Even for the most simple situation in which the optical fibre is surface mounted, problems may arise due to sliding between the cladding and coating in acrylic FBG sensors, that cause non-negligible measurement errors.

Although FBG based measurement systems have been successfully demonstrated in recent years and significant improvements, in particularly concerning the wavelength shift detection, have been achieved, there are still different metrological aspects, not yet adequately studied, that have to be considered for the practical application of the technique.

Depending on the coupling technique adopted (bonded or embedded fibre) and on the characteristics of the structural material, the in-plane and out-of-plane relative displacements between the sensor and the structure, if present, have to be evaluated. Furthermore, the influence of

the curvature radius of the structural component surface on the measured quantity is of interest: to the authors' knowledge this aspect has never been investigated and will be studied in the present article.

These factors could influence the metrological performance of FBG sensors and have to be taken into account through a careful calibration, for accurate measurements.

2. EXPERIMENTAL INVESTIGATION

The present paper deals with the characterization of a FBG sensor (type FBGS-1550-FC, Bragg Photonics Inc. having a centre wavelength CW = 1544 nm) whose total grating length is 14 mm, that was glued with an epoxy resin on specimens having increasing curvature in order to investigate the influence of curvature on the metrological performance of the sensor subjected to different loading conditions.

Preliminary free-bending tests, i.e. in absence of mechanical strain on the unbonded FBG sensor, have been conducted, showing no evidence of shift in wavelength of the returned Bragg signal, up to small curvature radius.

2.1. Design of the specimens and sensors lay-out

Different plane and curved specimens to be subjected to bending loads have been realised to investigate the response of the FBG transducer.

The material chosen for the specimen was aluminium (6061-T6). Two different specimen geometries have been considered:

- a 300 mm long beam with rectangular transversal section (width 30 mm, thickness 3 mm), subjected to four points bending load,
- 2 mm thick hollow tubes with axial length 110 mm, subjected to distributed lateral compression loads.

At this first stage of investigation, considering the total length of the Bragg grating over the FBG sensor, two hollow tubes having external diameters d_1=100 mm and d_2=50 mm, respectively, have been chosen on the ground of the results obtained, by means of an FE analysis, in terms of circumferential strain distribution. The flat beam subjected to four-points-bending load was chosen as reference (null curvature). It was instrumented with one FBG sensor and one strain gauge auto-compensated for aluminium (HBM 6/120 LY13, gauge factor K = 2,10 ±1%), placed on opposite sides of the plate, both aligned with the longitudinal axis of the plate, where uniform distribution of longitudinal strain is present according to the loading scheme adopted.

The two hollow tubes have been instrumented with different sensors (three HBM 6/120 LY13 strain gauges with K = 2,10 ±1% auto compensated for aluminium, and one FBG 1550-FC, Bragg Photonics Inc.) placed normally to the axis of symmetry.

The FBG sensor and SG#3 were centred at 90° degrees from the two loading surfaces of the testing machine as shown in Figs. 1 and 2. Strain gauges with active grid length of 14 mm were not commercially available, therefore the standard length 6 mm was chosen.

Strain gauge #1 and #2 (Fig. 2) were used to check the symmetry of the loading condition with respect to the transversal axis of both FBG sensor and strain gauge #3.

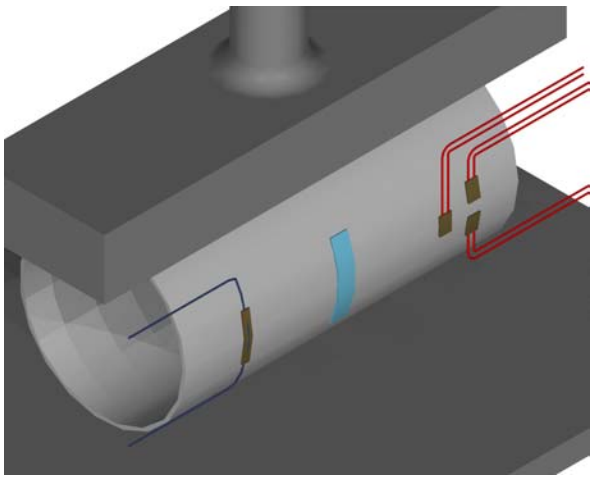

Fig. 1. Loading scheme: lateral compression of hollow tube

In addition, for the two hollow tube specimens, in order to check the displacement field induced on the specimen for each loading condition, shadow moiré images of the specimen area between the FBG sensor and the strain gauge's location have been recorded: shadow Moiré fringes represent iso-level contours on the surface under investigation.

The purpose is to show the actual curvature of the external surface of the specimen under the applied load. Shadow moiré uses the reference grating superimposed on its shadow to form a moiré pattern. This technique has the disadvantage that the master grating has a similar size to the measured object. Nevertheless in this paper, the use of shadow moiré [15-16] was preferred because the set-up is simple, robust and requires only a single image to obtain a three-dimensional measurement.

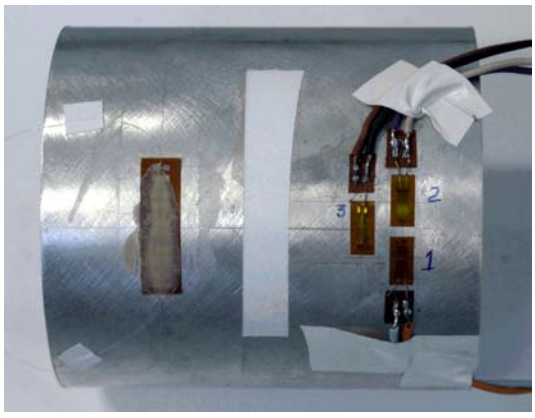

Fig. 2. Location of FBG and SGs on an hollow tube

The observed region for the shadow moiré was located in the space between the FBG and strain gauge #3.

This surface was painted white matt, as shown in Fig. 2, to enhance the greyscale contrast of the fringe pattern image.

2.2. Experimental setup

The utilized moirè setup consists of the following items: a 15 mW He-Ne illumination laser source, a moiré grid on glass plate (Graticules mod. SAG4) with rectilinear parallel fringes having a pitch *p* of 0,127± 0,0005 mm, a CCD B/W digital camera (SVS-Vistek CA085A10) (1280x1024 pixel), a camera lens (Nikkor AF Micro 70-210mm, 1:4 D), a Pentium class PC. The lay-out of the moiré set-up was characterised by a vision angle β=0 ±0,5° and a lighting angle α=37 ±0,5°.

The FBG interrogation system was a Micron Optics Inc. Fiber Bragg Grating Interrogation System (FBG-IS); it is a single channel system that can monitor up to 31 gratings utilizing a broadband source.

Fig. 3. Experimental setup

Strain gauge signals were measured by a Vishay Measurement Group P3500 strain indicator together with an SB-10 switch and balance unit. Theoretical standard uncertainty declared by equipment manufacturers is ± 4 µm/m (Micron Optics FBG-IS) and ±0,05% of the measured value ±3 µm/m (Vishay Measurement Group P3500).

FBG sensors were glued to the specimen utilising the following procedure: a polyamide carrier with a total length *l* = 25 mm is preliminarily bonded to the specimen surface using a typical cold-curing single-component adhesive (HBM Z70), the FBG sensor is then glued onto the polyamide carrier using a cold curing two component adhesive (HBM X60) based on acryl polymers.

No thermal sensitivity was considered as the laboratory environment where static test were performed was thermally conditioned with constant ambient temperature 20 ± 0.3 °C.

3. RESULTS AND DISCUSSION

The reference tests were performed on a 300 mm long beam with rectangular transversal section, subjected to four-points-bending load. The specimen was instrumented with an FBG sensor and a strain gauge, as described in the previous section.

Two different tests have been performed, the first one with the FBG subjected to tensile strain and the SG subjected to compression strain and the second one realized by placing the beam upside down so as to have the FBG sensor experiencing negative strain and conversely the SG experiencing positive strain. Each of these tests was repeated three times, showing good repeatability. Maximum experimental standard uncertainty of 7 ppm (SG measurements) and 17 ppm (FBG measurements) have been evaluated.

Results for both tests are shown in Fig. 4a and 4b, together with the regression lines obtained by applying the well-known least square method.

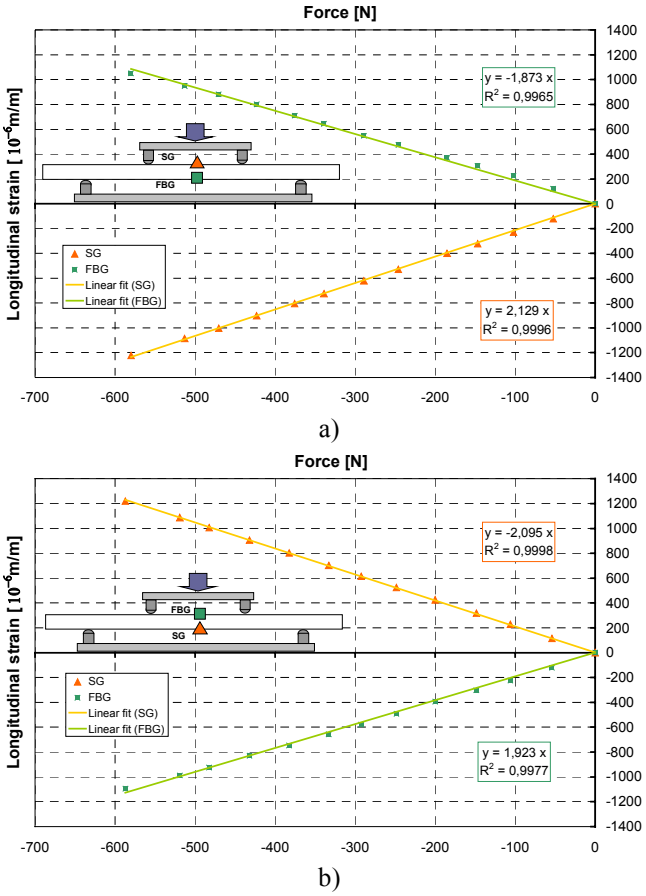

Fig. 4. a) four-points-bending test (FBG in tension) b) four-points-bending test (FBG in compression)

It can be observed that strains measured by the FBG sensor are always lower than those measured by the strain gauge (SG). Another result that should be pointed out is that the ratio between strain measured by the FBG and strain measured by the SG, is consistently higher for the tests where FBG is experiencing negative strain than for the tests where FBG is experiencing positive strain. These results are reported in Table 1 together with the corresponding results from tests performed on the 2 mm thick hollow tubes.

Preliminarily to the tests on the hollow tubes, a finite element analysis was performed, assuming an elastic linear behaviour of the material (6061-T6 with E = 71.000 MPa), on 100 mm and 50 mm diameter tubes subjected to lateral compression in order to calculate the tangential strain distribution along the circumference (i.e. for different circumferential positions). The obtained strain distribution shows a quasi-parabolic trend as shown in Fig. 5.

FBG and strain gauge #3, both located with the transversal axis of symmetry aligned with the cylinder generating line where the tangential strain is maximum, but

having an active length of 14 mm and 6 mm, respectively, will therefore sense a different mean strain value during the same loading step. In order to compare these measured strain values, a compensation coefficient was calculated on the ground of the numerical results reported in Fig. 5, to account for the reduced value of the tangential strain measured by the FBG sensor, owing to the greater length of its sensing grid compared to that of the strain gauge #3.

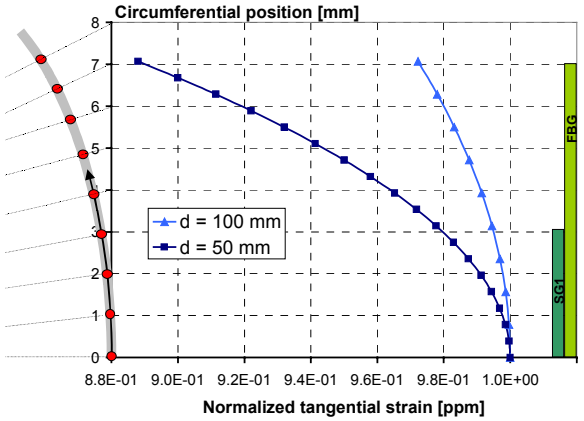

Fig. 5. Normalized tangential strains vs. circumferential positions on hollow tubes (FE analysis).

The calculated compensation coefficients are c_1= 1,008 for d_1 =100 mm and c_2= 1,032 for d_2 =50 mm. Strain measurement results for tests performed on cylindrical specimens with outer diameter 100 mm and 50 mm are illustrated in Figs. 6 and 7, respectively.

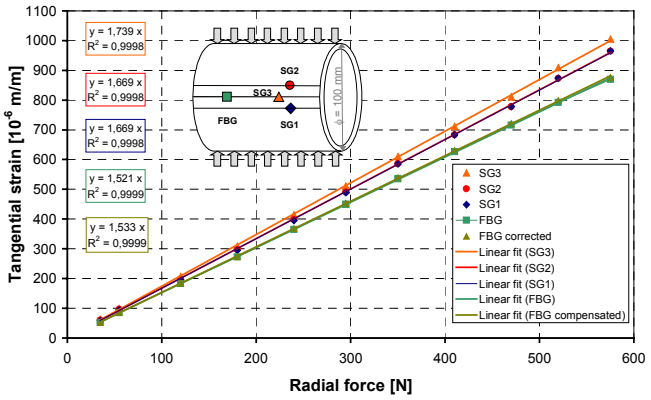

Fig. 6. Measured tangential strains vs. radial force (hollow tube with ϕ = 100 mm and 2 mm thickness).

In Fig. 6 both raw and compensated FBG measurements are given for the 100 mm specimen together with strain values measured by the three strain gauges. Maximum experimental standard uncertainty of ±6 ppm (SG measurements) and ±4 ppm (FBG measurements) have been evaluated. The good agreement of measurements from strain gauges #1 and #2 guarantees the correct loading condition which in turn assures the symmetry of the strain distribution around the transverse axes of symmetry of both FBG sensor and strain gauge #3. The comparison between FBG compensated measurements and strain gauge #3 measurements shows that FBG measures a lower strain value than that measured by the strain gauge. One possible explanation of this discrepancy can be ascribed to the presence of critical sliding effects between the cladding and coating in Acrylic FBG sensors that cause non negligible measurement errors because only a part of the total strain is transferred to the inner core that is the sensitive part of the FBG sensor; these effects are not of the stick-slip type but are rather proportional to the applied load. This phenomenon has already been observed by other researchers [6].

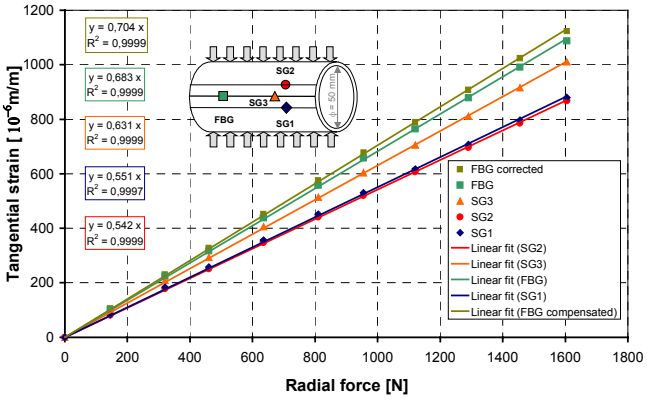

Fig. 7. Measured tangential strains vs. radial force (hollow tube with ϕ = 50 mm and 2 mm thickness).

In Fig. 7 the same curves as in Fig. 6 are plotted for the 50 mm diameter specimen. Maximum experimental standard uncertainty of ±4 ppm (SG measurements) and ±5 ppm (FBG measurements) have been evaluated. In contrast from what observed in the previous tests, the results from this test show clearly that strain measurements from FBG sensor are always larger than those obtained by the strain gauge. This happens although only a part of the total strain is transferred to the inner core of the FBG sensor owing to the action of the sliding effects observed both during the test on the 100 mm cylindrical specimen and during the four points bending test on the flat beam.

This test therefore highlights that the increase in the curvature of the surface where the FBG is bonded, can appreciably influence the response of the sensor.

The previous results are illustrated by the parameter obtained as the ratio of the FBG sensitivity vs. S.G. sensitivity calculated for each test condition described above, which is reported in Table I.

Table I. Ratio of FBG sensitivity vs. S.G. sensitivity

TEST	VALUE	NOTES
Flat specimen	0.92	FBG in compression
Flat specimen	0.88	FBG in tension
Hollow tube d= 100 mm	0.87	FBG in tension
Hollow tube d= 50 mm	1.08	FBG in tension

The following considerations can be made:

- the response of the FBG sensor can differ slightly depending on the positive or negative strain applied;
- no difference has been observed in the response of the positively strained FBG sensor when glued on flat beam or on surface with 50 mm curvature radius;
- the test performed on the hollow tube with curvature

radius 25 mm shows an opposite trend in the response of the FBG sensor whose output is now larger than that from the strain gauge.

A possible explanation for the different response of the FBG installed on the hollow tube with d_2 =50 mm compared with the hollow tube with d_1 =100 mm, has to take into account the different curvature of the specimens which is the only parameter that was changed.

This is strengthened by the fact that during both tests on hollow tubes the shape measurements made by the moiré technique have confirmed that curvature variations along the circumferential extension of the FBG sensor were not exceeding 0.013 mm from the initial value. It appears immediately in Fig. 8 from the observation of the fringe patterns recorded on both tubes before loading and after the final load was applied.

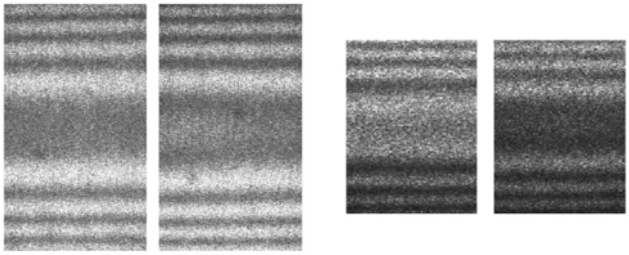

a) b)

Fig. 8. Moirè fringe patterns before and after loading a) 100 mm tube b) 50 mm tube

4. CONCLUSIONS

The behaviour of FBG strain sensors bonded on curved surfaces has been investigated. Two hollow tubes, having diameters 100 and 50 mm respectively, loaded in compression along two opposite generating lines, have been used for this purpose. Strain gauges were also applied as reference for tangential strain measurements. In addition, shadow moiré images of the specimen area between the FBG sensor and the strain gauge's location have been recorded to check the displacement field induced on the specimen.

Preliminary results obtained have shown that the FBG response (photo-elastic coefficient) depends on the curvature radius of the surface on which the sensor is bonded. This behaviour has never been observed until now, but, if confirmed in other tests, under different operative conditions, it will have to be considered for practical applications, in order to avoid large measurements errors. Another aspect that has been pointed out is the importance of an accurate calibration of the FBG sensor when it is bonded on a surface, because of the not negligible errors induced by the presence of sliding effects between the cladding and coating of the FBG sensor.

ACKNOWLEDGEMENTS

The Authors would like to acknowledge the precious support of Mr. A.M. Siddiolo in performing measurements. This work was carried out under the financial support of MURST (Italy), Cofin 2000, prot. MM09011855_004.

REFERENCES

[1] S. Huang, M. LeBlanc, M.M. Ohn, R.M. Measures, "Bragg intragrating structural sensing", *Applied Optics,* vol. 34, No. 22, pp. 5003-5009, 1995.

[2] Y.J. Rao, "In-fibre Bragg grating sensors", *Meas. Sci. Technol.*, vol. 8, pp 1442-1462, 1997.

[3] Y.J. Rao, "Recent progress in application of in-fiber Bragg grating sensors", *Optics and Lasers in engineering*, vol. 31, pp. 297-324, 1999**.**

[4] K.T.V. Grattan, T. Sun, "Fiber Optic sensor technology: an overview", *Sensors and Actuators A: Physical,* vol. 82, pp. 40-61, 2000.

[5] F.M. Haran, J.K. Rew, P.D. Foote, "A strain-isolated fibre Bragg grating sensor for temperature compensation of fibre Bragg grating strain sensor", *Meas. Sci. and Tech.,* vol. 9, pp. 1163-1166, 1998.

[6] G. Fanti "Thermo-mechanical characterization of fiber Bragg gratings sensors", *Proceedings of the V National Congress of Mechanical and Thermal Measurements*; Padua - Abano Terme, Italy, September 17-19, 2002.

[7] F.M. Araùjo, L.A. Ferreira, J.L. Santos, F. Farahi, "Temperature and strain insensitive bending measurements with D-type fibre Bragg gratings", *Meas. Sci. and Tech.,* vol. 12, pp. 829-833, 2001.

[8] M.J. Gander, W.N. MacPherson, R. McBride, J.D.C. Jones, L. Zhang, I. Bennion, P.M. Blanchard, J.G. Burnett, A.H. Greenaway, "Bend measurement using Bragg gratings in multicore fibres", *Electron Lett.,* vol.36, pp.120-121, 2000.

[9] B.A.L. Gwandu, X.W. Shu, Y. Liu, W. Zhang, L. Zhang, I. Bennion, "Simultaneous measurements of strain and curvature using superstructure fibre Bragg gratings", *Sens. Actuat. A* 96, pp.133-139, 2002.

[10] K. Lau, L. Yuan, L. Zhou, J. Wu, C. Woo; **"**Strain monitoring in FRP laminates and concrete beam using FBG sensors**";** *Composite structure ,* vol. 51, pp. 9-20, 2001.

[11] G.F. Fernando, T. Liu, P. Crosby, C. Doyle, A. Martin, D. Brooks, B. Ralph, R. Badcock, "A multi-purpose optical fibre sensor design for fibre reinforced composite materials", *Meas. Sci. Technol.,* vol. 8, pp. 1065-1079, 1997.

[12] L. Tang, X. Tao, C. Choy, "Effectiveness and optimisation of fiber Bragg grating sensor as embedded strain sensor", *Smart Mater. Struct.,* vol. 8, pp.154-160, 1999.

[13] K. Peters, P. Pattis, J. Botsis, P. Giaccari, "Experimental verification of response of embedded optical fiber Bragg grating sensors in non-homogeneous strain fields", *Optics and Lasers in Engineering,* vol. 33, pp. 107-119, 2000.

[14] W. Moerman, L. Taerwe, W. De Waele, J. Degrieck, R. Baets, "Reliability of Bragg grating strain sensors under cyclic and sustained loading", *Proc. of European Conference on System Identification & Structural Health Monitoring,* Madrid (E), pp. 531-538, June 2000.

[15] L.G. Melin, K. Levin, S. Nilsson, S.J.P. Palmer, P. Rae, "A study of the displacement field around embedded fibre optic sensors", *Composites Part A,* vol. 30, pp. 1267-1275, 1999.

[16] L. D'Acquisto, L. Fratini and A.M. Siddiolo, "A modified moirè technique for 3D surface topography", *Meas. Sci. and Tech.,* vol. 13, No. 4, pp.613-622, 2002.

Authors:

Leonardo D'Acquisto, Dipartimento di Meccanica, University of Palermo, V.le delle Scienze , 90128 Palermo, Italy – Phone: ++39 916657144, e-mail: dacquisto@dima.unipa.it

Roberto Montanini, Dipartimento di Chimica Industriale ed Ingegneria dei Materiali, University of Messina, Salita Sperone 31, 98166 Sant'Agata (ME), Messina, Italy – Phone: ++39 906765607, Fax: ++39 90391518, e-mail: rmontanini@ingegneria.unime.it